Climate forcing by carbonaceous and sulfate aerosols

Article *in* Climate Dynamics · October 1998

DOI: 10.1007/s003820050259 · Source: OAI

3 authors, including:

Keith Eric Grant
Ramblemuse Associates
84 PUBLICATIONS **2,233** CITATIONS
SEE PROFILE

C. C. Chuang
Lawrence Livermore National Laboratory
74 PUBLICATIONS **3,815** CITATIONS
SEE PROFILE

Climate Dynamics (1998) 14:839–851

J. E. Penner · C. C. Chuang · K. Grant

Climate forcing by carbonaceous and sulfate aerosols

Received: 29 September 1997 / Accepted: 10 June 1998

Abstract An atmospheric general circulation model is coupled to an atmospheric chemistry model to calculate the radiative forcing by anthropogenic sulfate and carbonaceous aerosols. The latter aerosols result from biomass burning as well as fossil fuel burning. The black carbon associated with carbonaceous aerosols is absorbant and can decrease the amount of reflected radiation at the top-of-the-atmosphere. In contrast, sulfate aerosols are reflectant and the amount of reflected radiation depends nonlinearly on the relative humidity. We examine the importance of treating the range of optical properties associated with sulfate aerosol at high relative humidities and find that the direct forcing by anthropogenic sulfate aerosols can decrease from $-0.81\ \mathrm{W\,m^{-2}}$ to $-0.55\ \mathrm{Wm^{-2}}$ if grid box average relative humidity is not allowed to increase above 90%. The climate forcing associated with fossil fuel emissions of carbonaceous aerosols is calculated to range from $+0.16$ to $+0.20\ \mathrm{Wm^{-2}}$, depending on how much organic carbon is associated with the black carbon from fossil fuel burning. The direct forcing of carbonaceous aerosols associated with biomass burning is calculated to range from -0.23 to $-0.16\ \mathrm{Wm^{-2}}$. The pattern of forcing by carbonaceous aerosols depends on both the surface albedo and the presence of clouds. Multiple scattering associated with clouds and high surface albedos can change the forcing from negative to positive.

J. E. Penner (✉)
Department of Atmospheric, Oceanic and Space Physics
University of Michigan, Ann Arbor MI, 48109-2143, USA
Fax: 734-764-5137
E-mail: penner@umich.edu

C. C. Chuang · K. Grant
Atmospheric Science Division, Lawrence Livermore National Laboratory, P.O. Box 808, L-170, Livermore, CA 94500, USA

1 Introduction

Radiative forcing by anthropogenic aerosols is recognized as an important contributor to climate change (IPCC 1996). The change in reflected radiation at the top-of-the-atmosphere due to the scattering and absorption of radiation by anthropogenic sulfate aerosols, termed the direct effect, has ranged from $-0.3\ \mathrm{Wm^{-2}}$ to $-0.9\ \mathrm{Wm^{-2}}$ in recent publications (Charlson et al. 1991; Kiehl and Briegleb 1993; Taylor and Penner 1994; Kiehl and Rodhe 1995; Chuang et al. 1997). Carbonaceous aerosols also are mainly produced by anthropogenic activities. They are composed of two components, black carbon (BC) and organic carbon (OC). Organic carbon from anthropogenic activities, like sulfate aerosol, is mainly scattering (e.g., Sloane et al. 1991; Novakov and Corrigan 1996; Hegg et al. 1997). Black carbon, on the other hand, is able to strongly absorb solar radiation; specific absorption coefficients are estimated to range from 7 to $12\ \mathrm{m^2\,g^{-1}}$ at 0.55 μm (Horvath 1993; Adams et al. 1989; Japar et al. 1986). This ability of black carbon to absorb radiation lowers the single scattering albedo of aerosols containing BC thereby reducing the amount of reflected radiation and increasing the amount of radiation absorbed by the atmosphere (Haywood and Shine 1995; Chylek and Coakley 1974). Therefore the presence of black carbon in aerosol may actually lead to a net heating of the atmosphere.

Here, we use an improved version of the coupled chemistry/atmospheric general circulation model of Chuang et al. (1997) to estimate the direct forcing by anthropogenic carbonaceous and sulfate aerosols (see also Taylor and Penner 1994 and the updated calculations in Penner et al. 1997a for a study of the climate effects of sulfate aerosols). The atmospheric general circulation model is derived from the NCAR CCM1 model (Williamson et al. 1987), but has an updated radiative transfer submodel that was specifically

developed to treat the scattering and absorption of solar radiation by aerosols (Grant et al. 1996; 1997 submitted). Here, we treat only the shortwave radiative forcing because carbonaceous and sulfate aerosols are mainly sub-micron in size and therefore have very small radiative cross sections at longer, thermal wavelengths (see also Haywood and Ramaswamy 1998). The atmospheric general circulation model is coupled to the GRANTOUR model which is used to predict aerosol concentrations (Penner et al. 1994; Liousse et al. 1996; Chuang et al. 1997). The previous applications of the GRANTOUR model include full comparisons of the model predictions of aerosol concentrations to available concentration and deposition data. In most cases and in most locales, the comparison with data is quite good. An exception is the model's prediction of BC near the poles which is too small relative to observed concentrations of BC (Liousse et al. 1996) and its prediction of sulfate aerosol in the winter season in Europe which is also too small (Penner et al. 1994). The model prediction of OC and BC is also lower than measured concentrations in the national parks in the USA, but it is not known whether this is a general fault of the US emissions inventories or whether the measured concentrations in the national parks are high relative to background concentrations due to local emissions of smoke. Because the polar regions are relatively small in spatial extent, the underprediction in this region should not have a large impact on hemisphere or global radiative forcing. Our calculated sulfate forcing, however, may be underestimated by perhaps a factor of 2 in winter over Europe.

Prior to this work, radiative forcing by anthropogenic carbonaceous aerosols has only been estimated using simplified models or models that neglect the scattering of solar radiation that is associated with organic aerosols (Penner et al. 1992; Penner 1995; Haywood and Shine 1995; Chylek and Wong 1995; Schult et al. 1997; Haywood and Ramaswamy 1998). As noted in several recent papers (Pilinis et al. 1995; Nemesure et al. 1995), the calculated aerosol forcing is very sensitive to the assumed aerosol size distribution as well as to the change in size distribution associated with increasing relative humidity. In this study, we fix the dry size for particles from various sources, but vary the optical properties consistent with the chemical nature of each aerosol using Köhler theory to estimate the magnitude of the change in size distribution associated with relative humidity changes. In addition to estimating forcing by carbonaceous aerosols, we reexamine the forcing by anthropogenic sulfate aerosols and show that because of the strong dependence of optical properties on relative humidity, the calculated forcing from any given climate model can vary substantially, depending on the treatment of humidity within the model.

2 Sources of carbonaceous and sulfur aerosols

Anthropogenic carbonaceous aerosols derive from two main sources: biomass burning and industrial activity. Here, we adopt the inventory for biomass aerosols developed by Liousse et al. (1996). The biomass burning processes considered by Liousse et al. (1996) included (1) savannah fires to clear and renew land, (2) forest fires for clearing purposes, (3) burning of agricultural waste to clear land, (4) the burning of wood to make charcoal and (5) the burning of wood, agricultural wastes, charcoal, and dung for fuel. Table 1 provides a summary of these emissions. Burning in temperature and boreal forests is also prevalent, but has not been considered here because most of this burning is the result of natural fires. Emissions from these fires might add between 2 to 4 Tg smoke y^{-1} to the totals shown in Table 1 (Stocks 1991; Vose et al. 1996; Wang et al. 1996; Cahoon et al. 1996).

The principal sources of black carbon from fossil fuel emissions derive from diesel fuel use and coal combustion (Penner et al. 1993; Cooke and Wilson 1996). On a global basis these emissions have been estimated from fuel use statistics as 6.6 Tg/y by Penner et al. (1993) and as 8.0 Tg/y by Cooke and Wilson (1996). In the following estimates of forcing, the inventory of Penner et al. (1993) has been used.

Emissions of organic carbon from fossil fuel use are not well known, but, typically the concentration of OC is larger than that of BC in urban areas (Bremond et al. 1989; Rogge et al. 1993). The source of this OC is not necessarily associated with the main sources of BC in any given urban area and some may originate from vegetation (Gray et al. 1984). In the absence of good emissions inventories for OC from urban and industrial activities, Liousse et al. (1996) used an estimate for the

Table 1 Sources of carbonaceous aerosol from biomass burning

	Total biomass burned (Tgdm/y[a])	Total smoke emissions (Tg/y)	BC emissions (Tg/y)
Savanna	2682	21.7	2.2
Forest	1259	22.7	1.9
Agricultural fires	564	4.45	0.53
Wheat and other grains	192	2.06	0.22
Corn	41.1	0.46	0.04
Rice	218.5	1.15	0.19
Sugar cane	112.4	0.78	0.09
Domestric fires	869.5	11.07	1.01
Wood and bagasse	752.4	8.88	0.88
Charcoal	16	0.16	0.02
Dung	101.1	2.02	0.10
Total	5374.5	59.9	5.64

[a]Tgdm is tetragrams of dry matter

ratio of OC to BC emissions from measured ratios of OC to BC in urban regions (which range up to 3.5 gC/gC) to define the range of possible emissions of OC from fossil/urban sources. Using a factor of 1.3 to convert from carbon to the molecular form of organic compound gave an estimated upper limit for these emissions of approximately 30 Tg/y. Here, in order to gauge the possible range in forcing by carbonaceous aerosols from fossil/urban sources we considered two cases. In the first, anthropogenic OC emissions are considered negligible and the forcing by fossil BC is calculated separately. In the second, the estimate of OC emissions from Liousse et al. (1996) are included together with BC emissions.

For sulfur, we used an emissions data base that was developed for calendar year 1980 (Penner et al. 1994). This emission inventory for SO_2 is $\sim$16% higher than that developed recently for 1985 (Benkovitz et al. 1996; compare Penner et al. 1994). However, the use of the 1980 inventory is consistent with our emissions data base for fossil BC and is also similar to the years for which our biomass burning inventory was developed (i.e., late 1970s).

3 Radiative properties of carbonaceous and sulfate aerosols

The radiative properties of the aerosol are determined by its size distribution and refractive index. The refractive index depends on the chemical nature of the aerosol. The chemical nature of the aerosol also determines whether it will take up water and grow in size with increasing relative humidity. We have modeled this behavior using the Köhler equations together with an assumed dry biomass, sulfate, or carbonaceous aerosol size distribution (Pruppacher and Klett 1978). For sulfate aerosol, we assumed the sulfate was present as $(NH_4)_2SO_4$ for these calculations. Smoke particles are made up of a variety of water-soluble salts and other elements. In our calculations for biomass aerosol, we assumed that their growth behavior was similar to that of an aerosol that was 30% $(NH_4)_2SO_4$ by mass (Chuang et al. 1992). BC from fossil fuel combustion is generally thought to be hydrophobic, but little is known about the hygroscopic behaviour of OC associated with fossil/urban emissions. Here, we ignore any uptake of water by industrial OC. All water uptake by industrial aerosols is then solely due to sulfate aerosols. This is a simplification because the water in an aerosol results not only from the presence of sulfate and ammonium in the aerosols, but is also due to nitrate and its associated compounds (Penner et al. 1997b). We are in the process of evaluating the effects of this simplification.

We used two size distributions in order to examine the range of forcings associated with the representation of biomass aerosols. The first distribution was that used by Chuang et al. (1992) to model smoke aerosols from a temperate fire. This distribution was based on measurements for the Hardiman fire by Radke et al. (1988). For the second distribution, we fit the average aerosol size distribution measured in the TRACE-A biomass experiment (Anderson et al. 1996) with the sum of 3 log-normal distributions. In keeping with the observations of Pereira et al. (1996), the largest mode was assumed to be dust, not smoke and this mode did not take up water with increasing relative humidity. For sulfate aerosol, following Kiehl and Briegleb (1993), we used a log-normal distribution with dry mode radius 0.05 μm and geometric standard deviation 2.0. In the absence of any good data for describing the size distribution of OC and BC from fossil fuel and urban emissions, we assumed the size distribution was the same as that from the Hardiman fire (Radke et al. 1988). Finally, as noted, we also treat one case in which anthropogenic OC is considered negligible. In order to calculate a specific extinction coefficient for BC that is within the range of measured specific extinction coefficients (Horvath 1993) when BC is assumed to be externally mixed from other aerosols, it is necessary to assume a size distribution that has a mode radius much smaller than the accumulation mode radii normally found for atmospheric aerosols. Here, we follow Haywood and Shine (1995) and adopt the size distribution from d'Almeida et al. (1991) for this calculation. Table 3 summarizes these dry distributions.

Table 2 Sources of carbonaceous and sulfate aerosols associated with fossil fuel/urban and industrial sources

	Emissions of BC (Tg/y)	Emissions of OC (Tg/y)[a]	SO_2 emissions (Tg S/y)
Fossel fuel and industry	6.64	30.2	75.7

[a]Assumed proportional to fossil fuel emissions of BC

Table 3 Size distribution parameters for distribution of sulfate and carbonaceous aerosols

Aerosol component	N_i[a]	r_i, μm	σ_i
Sulfate	1.0	0.05	2.0
BC	1.0	0.0118	2.0
Biomass-A[b]	0.9987	0.0774	1.402
	1.306×10^{-3}	0.3360	1.383
	2.830×10^{-4}	0.9577	1.425
Biomass-H[c]	0.428571	0.005	1.5
	0.571428	0.08	1.7
	1.e-6	2.5	1.65

[a]N_i is normalized by the total number concentration of aerosols and is dimensionless

[b]An approximate fit to the average distribution measured by Anderson et al. (1966)

[c]An approximate fit to the distribution measured for the Hardiman fire by Radke et al. (1988)

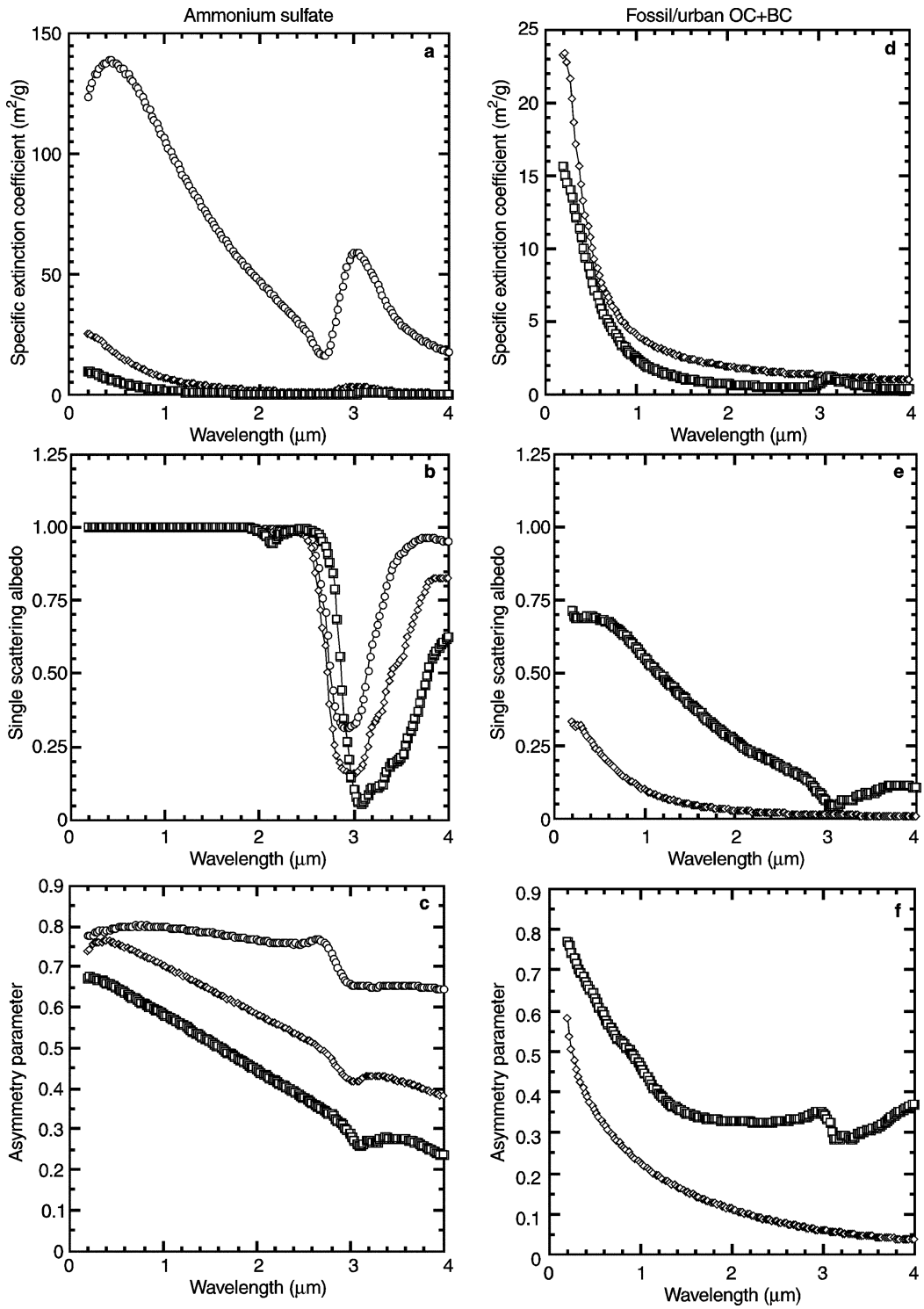

Fig. 1a–f Specific extinction coefficients, single scattering albedo and asymmetry parameters calculated for ammonium sulfate aerosol (**a**, **b**, **c**) and aerosols associated with fossil/urban OC + BC (**d**, **e**, **f**). For ammonium sulfate, we show these properties at 40% *RH* (*squares*), 80% *RH* (*diamonds*), and 99% *RH* (*circles*). For fossil/urban OC + BC, we show the optical properties associated with treating BC only (*diamonds*) and OC + BC (*squares*)

As noted by Liousse et al. (1996) aerosols from biomass burning contain a varying ratio of BC to total mass in the smoke. To account for their varying optical properties in the calculation of radiative forcing, we developed the scattering and absorption properties for these aerosols by first calculating the size distribution as a function of relative humidity and BC fraction. Then, we took the volume average of the refractive

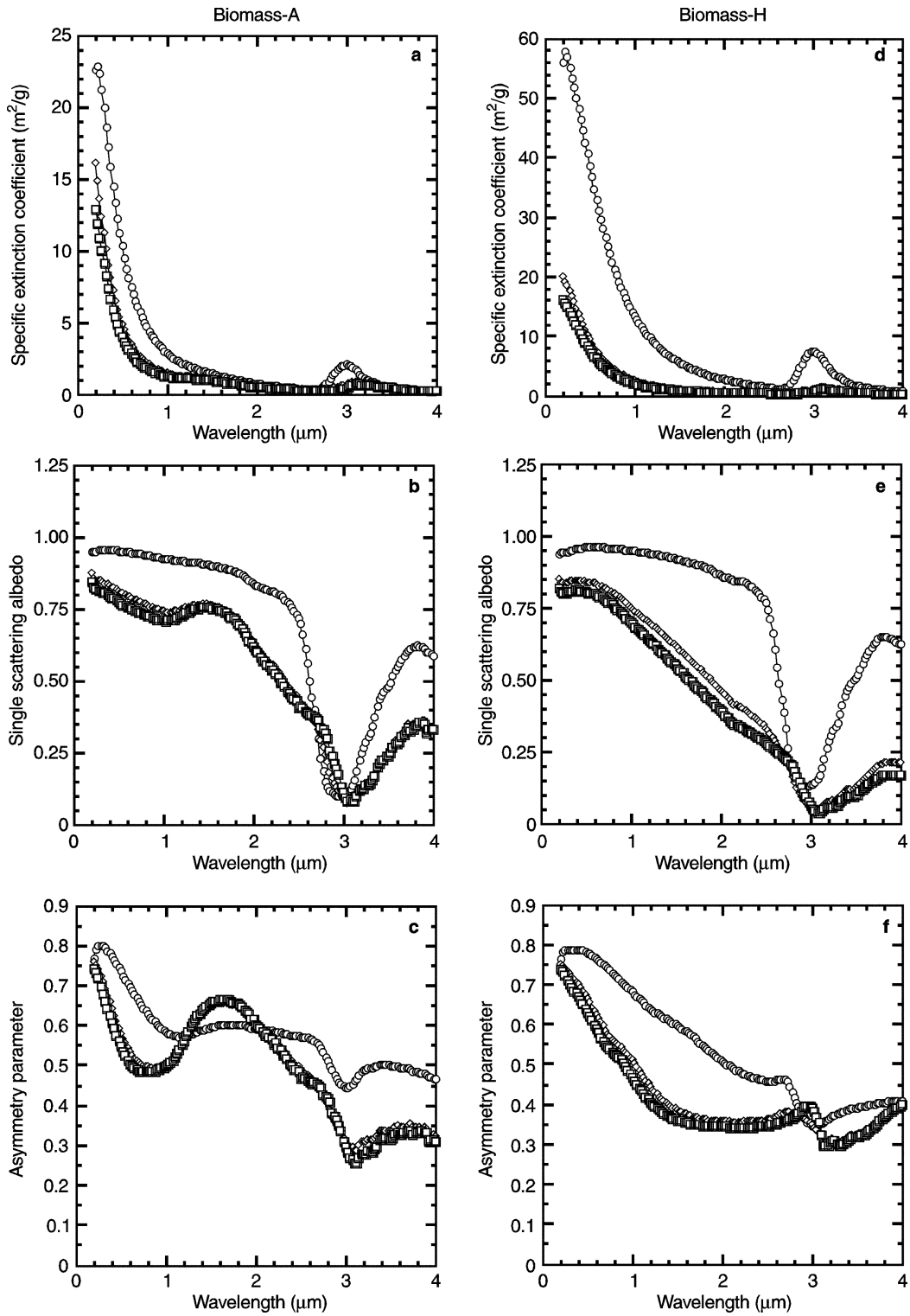

Fig. 2a–f Specific extinction coefficients, single scattering albedo and asymmetry parameters calculated for biomass aerosols using the Anderson et al. (1996) size distribution (**a**, **b**, **c**) and **d–f** using the Hardiman fire distribution (Radke et al. 1988). Each figure shows the calculated properties at 40%*RH* (*squares*), 80% *RH* (*diamonds*), and 99% *RH* (*circles*)

index for each component of the aerosol and calculated the specific scattering and absorption coefficients and asymmetry factor from Mie theory. These values formed a matrix giving the optical properties at any RH, BC fraction and wavelength. A similar procedure was followed for developing the optical properties of sulfate aerosol as a function of relative humidity. For convenience in our parameterization, we assigned the refractive

Table 4 Optical properties for dry aerosols (40% *RH*) at 0.55 μm

Aerosol type	σ_s(m^2 g^{-1})		σ_a (m^2 g^{-1})		σ_s (80)/σ_s (dry)	
	Modeled	Observed	Modeled	Observed	Modeled	Observed
Biomass-A	2.5[a]	2.8–3.3[b]	0.78[a]	0.62–0.83[b]	1.29	1.10–1.37[b]
Biomass-H	5.18[c]	2.6–6.0[d]	1.30[c]	0.36–0.82[d]	1.30	
Fossil OC + BC	4.84	3.9–4.1[e] 1.5–8.0[f]	2.32	1.3–2.2[g]	na	
Fossil BC	1.94	2–3[h]	7.34	7–12[h]	na	
Ammonium Sulfate	5.07[i]	2.3–6.8[f]	0.00		3.10	

[a]Developed using the size distribution measured by Anderson et al. (1996)
[b]From Hobbs et al. (1997) in South American fires
[c]Developed using the Hardiman fire size distribution measured by Radke et al. (1988)
[d]From Radke et al. (1988) for temperate forest fires
[e]From Hegg et al. (1997). This is the scattering per unit gram of C in aerosol and must be multiplied by an unknown factor to arrive at the scattering per unit mass of OC + BC
[f]Zhang et al. (1994)
[g]The measured range was calculated using a range of 7–12 m^2/g for the specific absorption of BC together with the BC to total mass of OC assumed here (~ 0.2)
[h]Horvath (1983); Adams et al. (1989); Japar et al. (1986); Groblicki et al. (1981).
[i]m^2/g of $SO_4^=$. This includes the water of hydration at 40% RH that is associated with $SO_4^=$

index for ammonium sulfate to both sulfate and organic carbon aerosols (Toon et al. 1976) and the refractive index for soot to black carbon aerosols (Fenn et al. 1985). The large component for the Anderson et al. (1996) size distribution was assigned the refractive index for dust (Fenn et al. 1985). Figure 1 shows the extinction coefficient, single scattering albedo, and the asymmetry parameter developed in this manner for the sulfate and fossil/urban OC and BC while Fig. 2 shows these properties for the two distributions associate with biomass aerosols (we assumed an average BC fraction for biomass aerosol of 10% for these figures). Table 4 compares our calculated values to measured values. For sulfate and biomass aerosols the calculated optical properties at 80% and 99% relative humidity are also shown in the figure. Note the very substantial increase in extinction coefficient at large relative humidity especially for the sulfate aerosols. As we show later, the large increase in extinction coefficient above 90% RH can lead to significant enhancements in the calculated total forcing by the aerosol. Figure 2 also shows a significant response in our calculated extinction coefficients associated with biomass aerosols at high relative humidity.

4 Radiative treatment

Our radiative calculations use a two-stream algorithm with an adding method to account for multiple scattering (Liou 1980; see also Grant and Grossman 1998). A spherical atmosphere treatment is used for the direct solar beam at large solar zenith angles, while a plane parallel treatment is used for multiple scattering. Sources of diffuse radiation are calculated using the delta-Eddington algorithm (Grant et al. 1996). To properly capture the variation of aerosol properties with ozone absorption and Rayleigh scattering requires the use of nine bands in the ultraviolet and visible wavelengths (0.175–0.7 μm) while three bands are sufficient in the near-infrared (0.7–4 μm) (Grant et al. 1997). The optical properties from our detailed Mie calculations were averaged over the wavelength bands in our radiative transfer model, weighted by the solar energy available at each wavelength within the bands.

The model calculation of forcing proceeded in the following manner. The chemical transport model was used to calculate aerosol concentrations every 6 h. These were passed to the atmospheric general circulation model which was used to calculate the top-of-atmosphere and surface forcing as the difference between the net shortwave flux with and without anthropogenic aerosols. This procedure assures that the cloud distribution remains precisely the same for the calculation with and without aerosols, thereby assuring an accurate evaluation of forcing in spite of the fact that it is a small difference between two large numbers. The treatment of aerosol scattering and absorption inside clouds deserves some discussion. Sulfate and biomass aerosols are known to be good cloud condensation nuclei (CCN) and, therefore, they are not included in the radiative transfer calculation inside clouds (they are part of an "indirect effect"). It is unknown whether fossil/urban sources of OC and BC would independently act as CCN, but they certainly will do so once associated with sulfur. However, here, we treat them as distinct from sulfur and therefore include scattering and absorption by OC + BC within cloud. Below we tested how large a change in forcing results from this assumption.

5 Results

Figure 3a shows the annually averaged forcing by biomass aerosols. In this calculation the optical properties that were calculated with the size distribution measured by Anderson et al. (1996) were used. Biomass aerosol forcing is strongest in the tropics, where it is mainly negative. However, regions of positive forcing

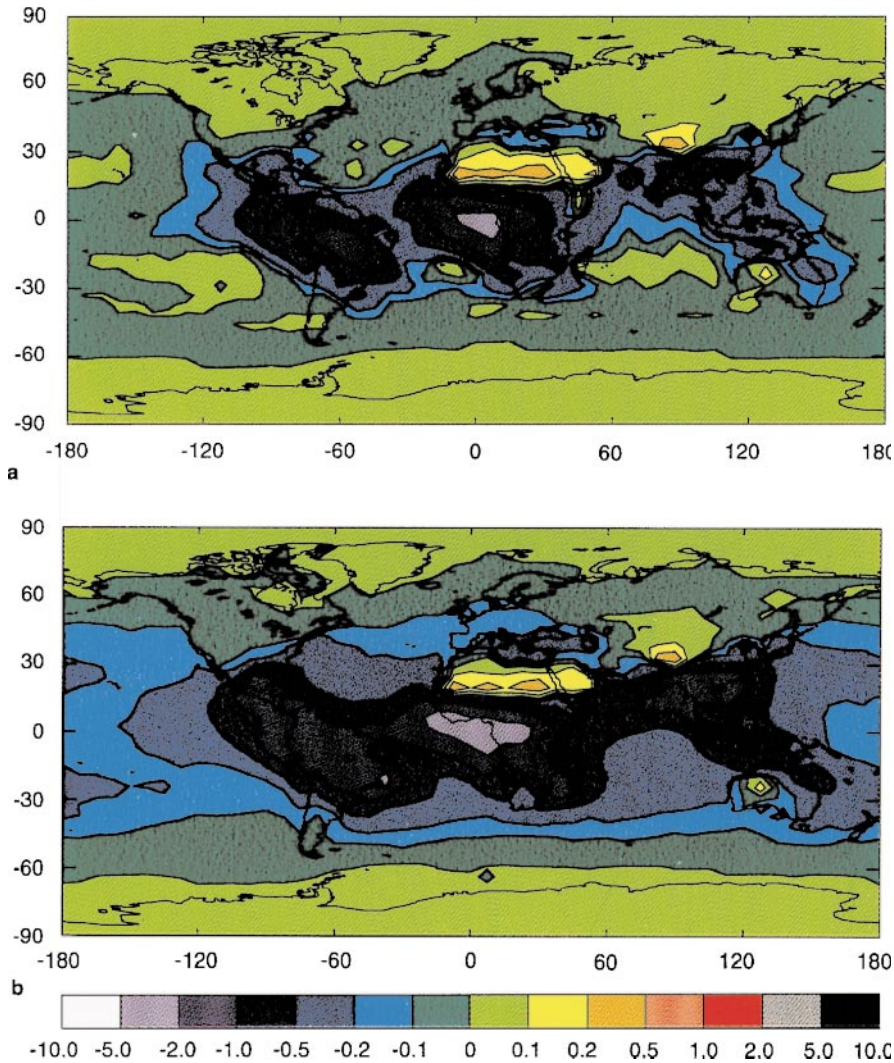

Fig. 3a, b Calculated forcing (in Wm^{-2}) for biomass aerosols assuming the Anderson et al. (1996) size distribution for **a** whole-sky and **b** clear-sky only

are present over the Sahara desert as well as over some ocean patches between 10°N and 30°N and between 10°S and 50°S. Positive forcing is also evident over land areas poleward of about 30°. Over areas of high surface albedo, the net effect of absorbing aerosols is a warming (Haywood and Shine 1995), and this effect is clearly responsible for the calculated positive forcing over the Sahara. Enhanced positive forcing is also expected over darker surface albedos if clouds overlay or underlay the aerosols. This is because the multiple scattering induced by the cloud allows more absorption to take place within the aerosol layer below and above the cloud. To show this, we plot in Fig. 3b the clear sky forcing calculated for the same biomass aerosol distribution. Over all ice-free ocean areas and over most land areas not covered by ice, the forcing is negative. Therefore, the effects of clouds are to enhance the warming caused by carbonaceous aerosols.

The annually averaged forcing from biomass aerosols using the optical properties associated with the Anderson et al. (1996) distribution is $-0.16\ Wm^{-2}$. The Radke et al. (1988) distribution results in an increased (negative) forcing as expected from the scattering and absorption coefficients calculated for this aerosol (see Table 4 and Fig. 2). The annual average forcing increases to $-0.23\ Wm^{-2}$ while the pattern of forcing is very similar to that in Fig. 2a. The increase in forcing magnitude is somewhat smaller than the increase in dry scattering or extinction coefficients at visible wavelengths and considerably smaller than the increase in extinction coefficients at high relative humidity. This non-linear response in the net shortwave flux at the top of the atmosphere is due to the absorbing nature of these aerosols. As more scattering material is added or as scattering coefficients are increased, absorption also increases due to enhanced multiple scattering

In these calculations, aerosol in cloudy regions was not included in the radiative transfer calculation because biomass aerosols should be good CCN and contribute to indirect forcing. However, as a sensitivity test, we also considered a case where the biomass aerosols were assumed to be externally mixed within cloudy

regions. In this case the magnitude of the forcing is decreased from -0.16 to -0.14 Wm^{-2} (Table 5). The multiple scattering which occurs within cloudy areas allows more absorption by the biomass aerosols, but the effect appears to be small.

Figure 4a, b shows the forcing by fossil fuel BC alone and that by the combined fossil/urban OC + BC, respectively. The calculated annual average forcing for these two cases is $+0.20$ Wm^{-2} and $+0.16$ Wm^{-2}, respectively. These forcings are mainly associated with emissions in North American, Europe and Asia and the spatial extent is similar to that from sulfate aerosol (see Fig. 5). For BC alone, the low single scattering albedo for this aerosol (Fig. 1) leads to the expectation that forcing should be positive everywhere as it is. For fossil/urban OC + BC, because the single scattering albedo of this aerosol type is between 0.6 and 0.7 for wavelengths less than 1.0 μm, the forcing is also positive almost everywhere. Small regions of negative forcing occur over regions with low albedo (water surfaces). This negative forcing is as high as -0.5 Wm^{-2} over regions with high optical depths such as over the Mediterranean Sea. To see the effects of clouds enhancing absorption, Fig. 4c shows the clear sky forcing by fossil/urban OC + BC. As shown here, most of the positive forcing over ocean regions in Fig. 4b is due to the presence of clouds and the additional multiple scattering and absorption which they induce.

Figure 5 shows the pattern of direct forcing by sulfate aerosols. This pattern and magnitude of total forcing (-0.8 Wm^{-2}) is similar to that calculated in Taylor and Penner (1994) but twice the magnitude calculated by Chuang et al. (1997). The similarity with Taylor and Penner (1994) is a coincidence which results from the fact that here we use the full range of sensitivity to relative humidity (see Fig. 1a), while in the previous calculation, we used a fixed relative humidity with an extinction coefficient of 8.5 m^2/g over a broader range of visible wavelengths. To examine the effect of allowing the particles to grow up to their full size at 99% *RH*, we performed a separate calculation where the particle size and optical properties remain fixed at those associated with $RH = 90\%$ if the relative humidity was higher than 90%. In this calculation the forcing decreased by 50% (to -0.53 Wm^{-2} see Table 5) similar to the value we calculated previously when the *RH* dependence was capped above 90% (Chuang et al. 1997). This demonstrates the importance of defining the spatial extent of regions with high relative humidity in order to properly include aerosol forcing in climate models, a point also stressed by Haywood et al. (1995). The latter authors compared the forcing obtained with a limited area model with high spatial resolution and the capability to resolve areas of high relative humidity with that found using a GCM parametrization over a course grid. They found their GCM parametrization underestimated the direct forcing by $\sim 60\%$. In this climate model we allow *RH* to reach 100% over an entire grid box before forming cloud and removing water by precipitation (Taylor and Ghan 1992). This procedure may partially offset the inability of the GCM to properly resolve areas of high relative humidity. On the other hand, this procedure may lead to an overestimate of the forcing by sulfate aerosols. We note that separate calculations of the direct forcing by sulfate aerosols which use this same methodology and the ECHAM climate model are substantially smaller than the present results (Molenkamp et al. in preparation 1998).

Table 5 Top-of-atmosphere shortwave forcing by sulfate and carbonaceous aerosols (Wm^{-2})

Case	Northern Hemisphere	Southern Hemisphere	Global average
Biomass-A	−0.14	−0.18	−0.16
Biomass-H	−0.20	−0.26	−0.23
Biomass-A (external mixing)	−0.12	−0.16	−0.14
Fossil/urban OC + BC	+0.31	+0.01	+0.16
Fossil BC	+0.37	+0.02	+0.20
Sulfate	−1.18	−0.26	−0.81
Sulfate (*RH* < 90%)	−0.88	−0.17	−0.53
Sum of forcing[a]	−0.65 to −1.07	−0.33 to −0.51	−0.49 to −0.88

[a]The lower limit is the sum of sulfate forcing (*RH* < 90%), fossil BC forcing, and biomass burning using the distribution measured by Anderson et al. (1996). The upper limit uses the full range of humdities for calculating the sulfate forcing, includes OC in the calculation of fossil/urban OC + BC, and assumes the Hardiman fire size distribution for biomass burning

Figure 6 shows the monthly average forcing for the Northern Hemisphere, Southern Hemisphere and global average for each of the aerosol cases examined here. The Northern Hemisphere forcing by sulfate aerosols is strongly negative and peaks in July as expected for a photochemically formed aerosol type that is dominant in the Northern Hemisphere. Surprisingly, forcing by sulfate aerosols also dominates the Southern Hemisphere during October through April. During this period biomass burning is low while fossil and industrial emissions of SO_2 are continuing throughout the year. The forcing by biomass aerosols in the Northern Hemisphere is smaller than that in the Southern Hemisphere, mainly because of the presence of absorbing areas over the Sahara in the Northern Hemisphere gives an area averaged forcing that is smaller than that in the Southern Hemisphere. Forcing by fossil fuel emissions of black carbon and associated OC is positive, but small, and mainly associated with areas of high domestic coal use and diesel fuel use in the Northern Hemisphere. This net positive forcing is small relative to the negative

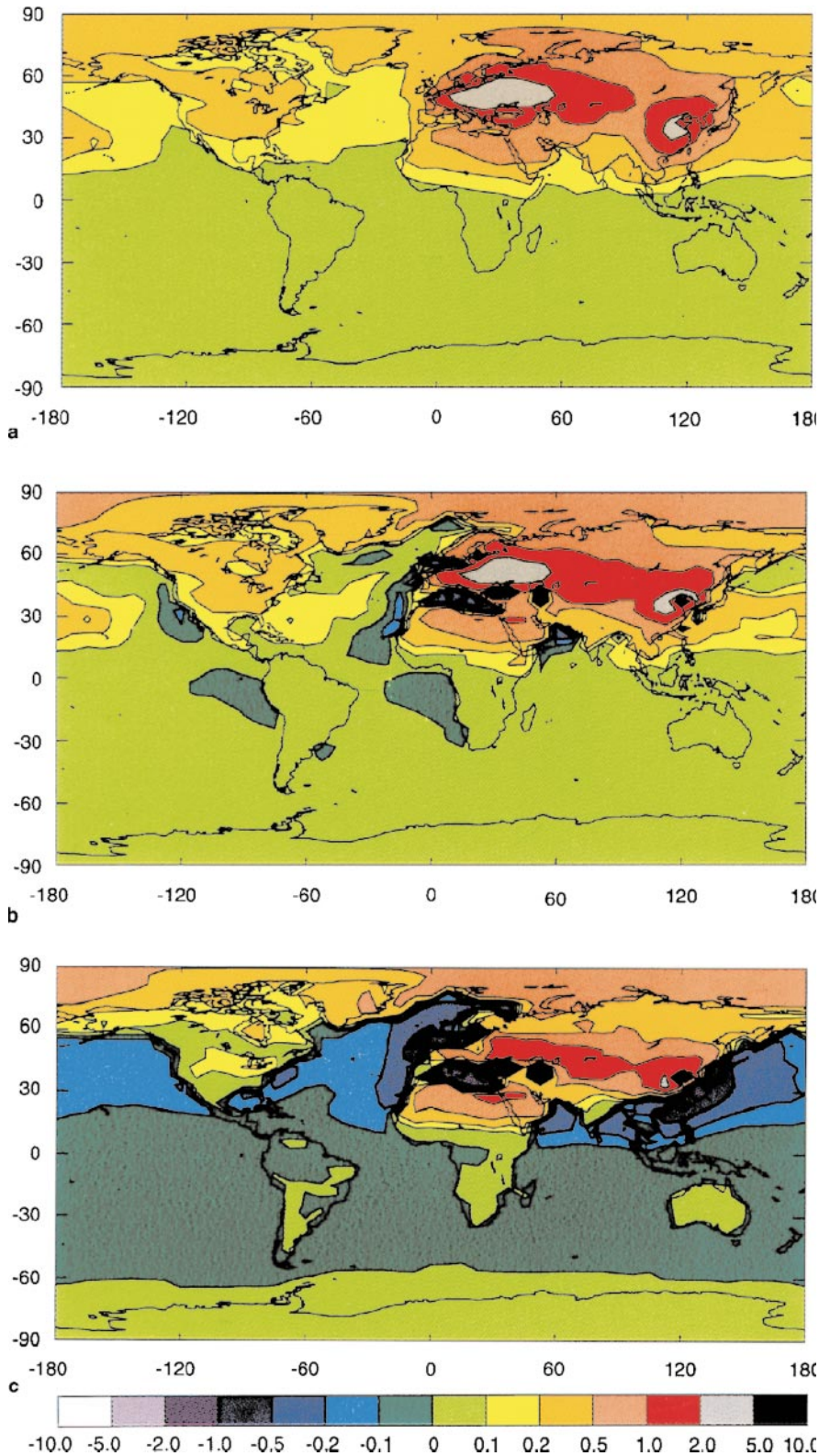

Fig. 4a–c Calculated whole-sky forcing (in Wm^{-2}) for **a** fossil fuel BC treated separately and **b** for fossil/urban OC + BC. **c** Shows the calculated forcing for clear-sky only for fossil/urban OC + BC

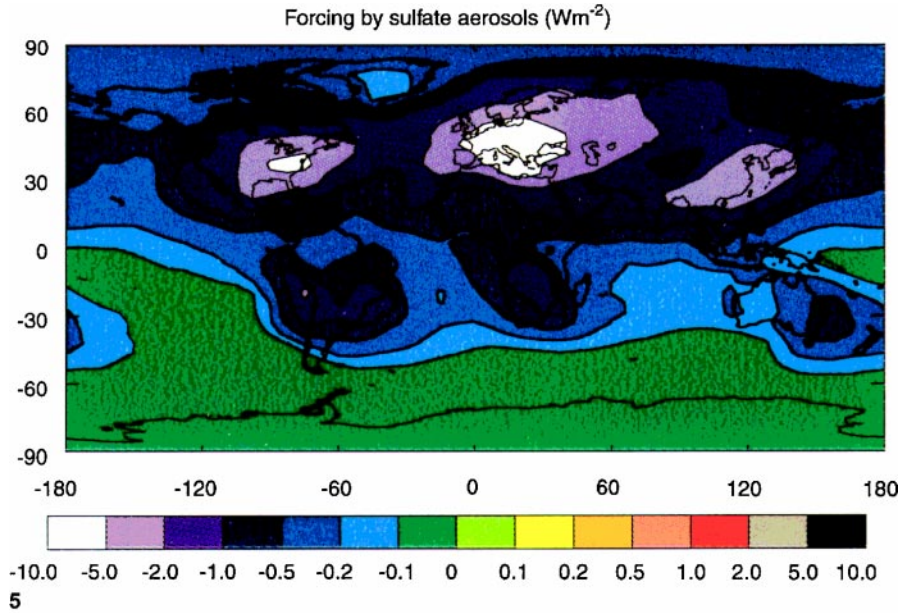

Fig. 5 Calcuated forcing (in Wm^{-2}) associated with sulfate aerosols

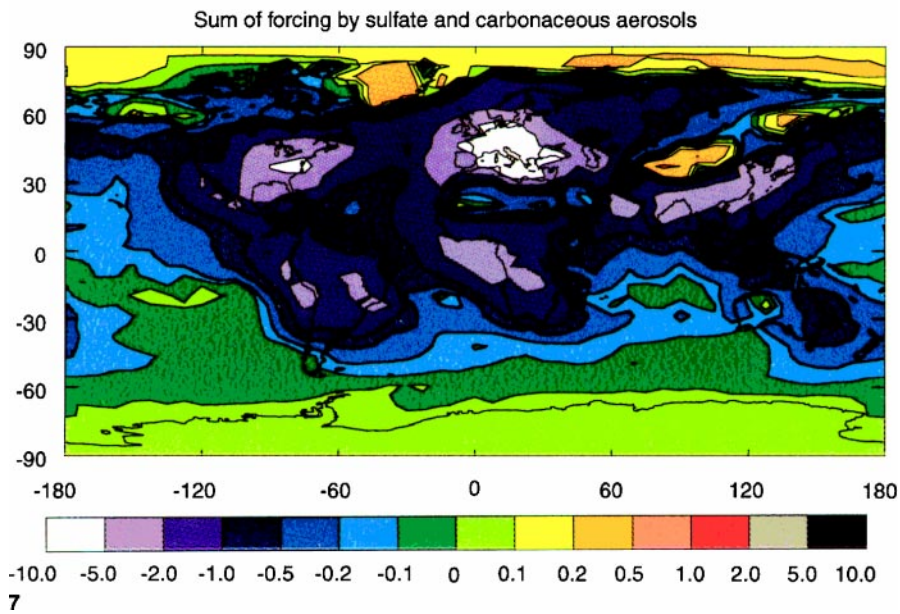

Fig. 7 The sum of forcing (in Wm^{-2}) associated with sulfate and carbonaceous aerosols. This figure was constructed by adding the forcing from biomass aerosols associated with the Anderson et al. (1996) distribution, the forcing by fossil OC + BC, and the forcing by sulfate aerosols assuming they respond to the full distribution of relative humidities calculated in the climate model

forcing by sulfate aerosol during the Northern Hemisphere summer but approaches that for sulfate aerosol in winter.

Figure 7 shows the sum of the forcing from all aerosol types considered here. For this figure we used the Anderson et al. (1996) size distribution for biomass aerosols and used the internal mixture for OC + BC from fossil/urban emissions. The presence of absorbing aerosols has decreased the spatial extent of negative forcing by sulfate aerosol but not to any large extent. However, over a small region in Asia and at high ice-covered latitudes, the net forcing is positive. Also, the negative forcing by biomass aerosols in the tropics is enhanced due to the additional forcing by sulfate in those regions.

6 Summary and discussion

We find that biomass aerosols act to cool the Earth/atmosphere system by between -0.16 and $-0.23\ Wm^{-2}$, while black carbon and associated

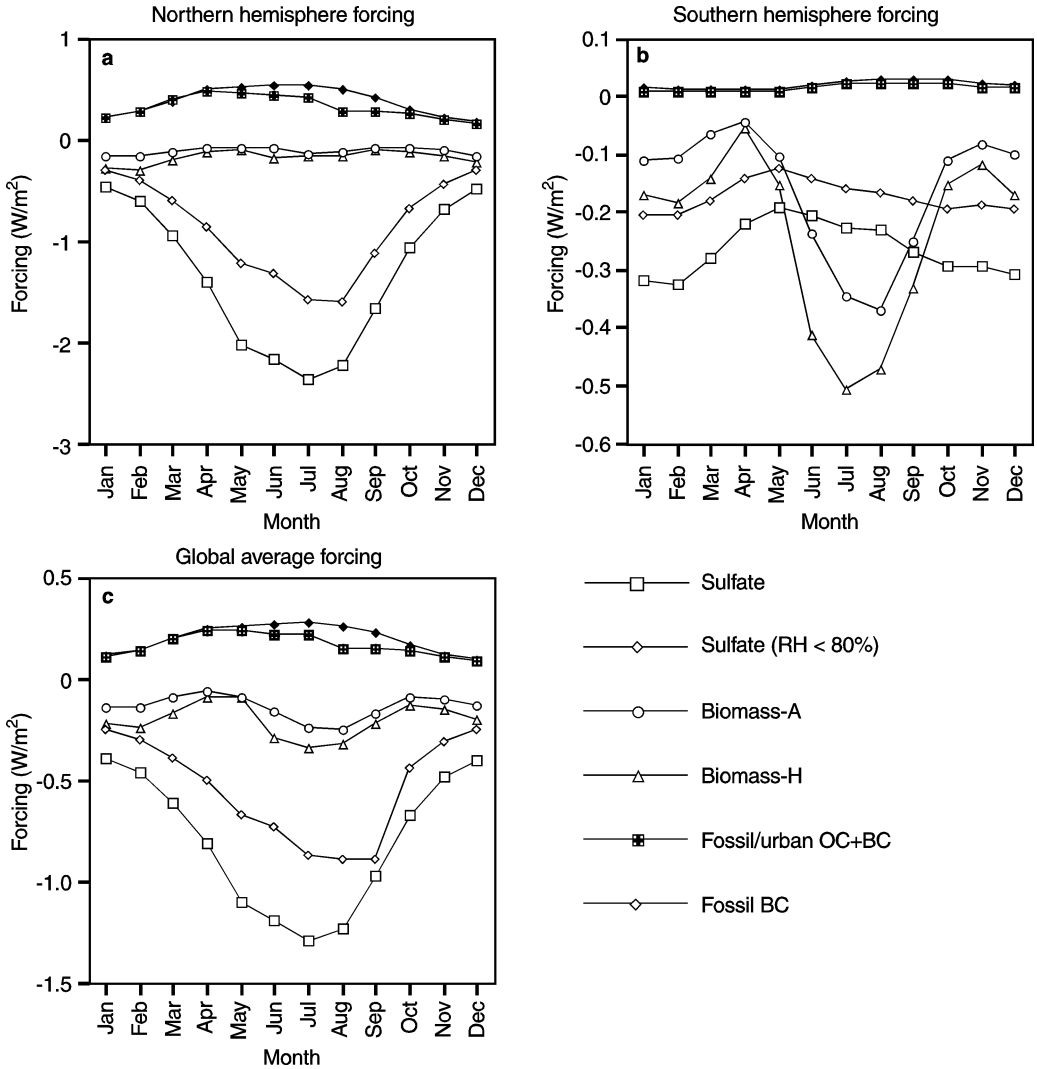

Fig. 6 a Northern Hemisphere, **b** Southern Hemisphere, and **c** global average forcing associated with each of the cases considered here

organic carbon from fossil fuel/urban sources acting alone may heat the system by between 0.16 and 0.20 Wm^{-2}. This net positive forcing is, however, balanced on average by a large negative forcing associated with sulfate aerosols. This negative forcing ranges from -0.53 to -0.81 Wm^{-2} on an annual average basis in our model and dominates the positive forcing by fossil BC, particularly in the Northern Hemisphere summer. The sum of the forcing by fossil BC, OC and sulfate ranges between -0.35 and -0.65 Wm^{-2}. These estimates for the effects of BC and OC aerosols from fossil fuels have assumed that BC and sulfate remain externally mixed. As noted by Haywood and Shine (1995), an internal mixture of BC and sulfate would increase the amount of absorbed radiation, and could decrease the overall net forcing by 20 to 60%. Applying this correction to our estimates would change the range of forcing by fossil BC, OC and sulfate to -0.14 to -0.52 Wm^{-2}. Table 5 summarizes the range of forcing calculated here from all aerosols (i.e., the sum of sulfate, biomass and fossil/urban OC + BC). The global average forcing is between -0.49 and -0.88 Wm^{-2}. If biomass and fossil/urban BC + OC and sulfate are internally mixed these estimates might decrease to -0.30 to -0.75 Wm^{-2}.

Our estimates for the direct forcing by carbonaceous and sulfate aerosols have assumed that these aerosols do not affect the circulation and average meteorology. However, absorbing aerosols heat the atmosphere itself, and may lead to a change in lapse rate or cloud cover. In Table 6 we summarize the amount of absorbed radiation in our calculations. Total absorbed radiation from carbonaceous aerosols (biomass + fossil/urban OC + BC) ranges from 1.31 Wm^{-2} to 2.11 Wm^{-2} on an annual average basis. Due to the effects of multiple scattering, we find more absorption within the atmosphere for more highly scattering mixtures of OC + BC. Thus, the absorbed radiation for the Radke et al. (1988) biomass distribution is higher than for the Anderson distribution even though the forcing at the top of the atmosphere by the former is more negative. Likewise, the absorbed radiation is higher for

Table 6 Radiation absorbed in the atmospheric column (Wm^{-2})

	Northern Hemisphere	Southern Hemisphere	Global average
Biomass-A	0.76	0.74	0.75
Biomass-H	1.22	1.16	1.19
Biomass-A (external)	0.81	0.79	0.80
Fossil/urban OC + BC	1.75	0.09	0.92
Fossil BC	1.06	0.05	0.56

the fossil/urban OC + BC than for BC alone, even though the (positive) forcing at the top of the atmosphere by OC + BC is smaller than that for BC alone.

The lowest estimates of direct forcing developed here may result in only a small climate impact, in contrast to estimates from previous studies which have ignored absorbing aerosols (Taylor and Penner 1994; Mitchell et al. 1995; Roeckner et al. 1995). On the other hand, estimates for the effect of indirect forcing (wherein aerosols modify cloud droplet radius and possibly lifetime) remain large and are far more uncertain than the estimates for direct forcing. Thus, for example, Chuang et al. (1997) used a mechanistic model to estimate the number of cloud condensation nuclei (CCN) and droplets formed as a result of anthropogenic sulfate emissions. They estimated that the forcing associated with a change in droplet size ranged from $-0.4\ Wm^{-2}$ to $-0.8\ Wm^{-2}$. These estimates accounted for that fact that most sulfate is formed within cloud droplets and does not cause an increase in CCN. Penner et al. (1996) made a preliminary estimate for the indirect forcing associated with increasing CCN due to carbonaceous aerosols which, unlike sulfate aerosols, may add CCN proportional to their emissions. This forcing ranged from $-2.5\ Wm^{-2}$ to $-4.5\ Wm^{-2}$. Furthermore, Lohman and Feichter (1997) calculated the possible change in forcing associated with a change in the lifetime and spatial extent of the clouds as a result of sulfate aerosols that ranged from $-1.5\ Wm^{-2}$ to $-4.5\ Wm^{-2}$. The Lohman and Feichter estimate may be too large because they did not include a mechanistic treatment for the change in CCN and initial droplet concentration while the Penner et al. estimate of indirect forcing by carbonaceous aerosols may be too large because they did not include absorption by BC within cloud drops and may need to consider higher natural emissions of organic aerosols. However, if these high negative forcings are confirmed through further study, they would imply that either we are missing some positive forcing mechanism or that the observed increase in surface temperature over the last 100 years has nothing to do with greenhouse gases. Clearly further study of this issue is needed.

Acknowledgements Work at Lawrence Livermore National Laboratory was performed under the auspices of the U.S. Department of Energy under contract W-7405-ENG-48. We are grateful for support from the NASA Atmospheric Chemistry and Analysis Program, the DOE Atmospheric Chemistry Program, and the DOE ARM Program. Computer time was supplied by the National Energy Research Super Computer Center.

References

Adams KM, Davis LI Jr, Japar SM, Pierson WR (1989) Real-time, in situ measurements of atmospheric optical absorption in the visible via photoacoustic spectroscopy. II. Validation for atmospheric elemental carbon aerosol. Atmos Environ 23:693–700

Anderson BE, Grant WB, Gregory GL, Browell EV, Collins JE Jr, Sachse GW, Bagwell DR, Hudgins CH, Blake DR, Blake NJ (1996) Aerosols from biomass burning over the tropical South Atlantic region: distributions and impacts. J Geophys Res 101:24 117–24 138

Benkovitz CM, Scholtz MT, Pacyna J, Tarrasón L, Dignon J, Voldner EC, Spiro PA, Logan JA, Graedel TE (1996) Global gridded inventories of anthropogenic emissions of sulfur and nitrogen. J Geophys Res 101:29 239–29 253

Brémond MP, Cachier H, Buat-Ménard P (1989) Particulate carbon in the Paris region atmosphere. Environ Tech Lett 10:339–346

Cahoon DR Jr, Stocks BJ, Levine JS, Cofer WR III, Barber JA (1996) Monitoring the 1992 forest fires in the boreal ecosystem using NOAA AVHRR satellite imagery. In: J Levine (ed) Biomass burning and global change. vol **2**, MIT Press, Cambridge, MA, pp 795–801

Charlson RJ, Langner J, Rodhe H, Leovy CB, Warren SG (1991) Perturbation of the Northern Hemisphere radiative balance by backscattering from anthropogenic sulfate aerosols. Tellus 43AB:152–163

Chuang CC, Penner JE, Edwards LL (1992) Nucleation scavenging of smoke particles and simulated droplet size distributions over large fires. J Atmos Sci 49:1264–1275

Chuang CC, Penner JE, Taylor KE, Grossman AS, Walton JJ (1997) An assessment of the radiative effects of anthropogenic sulfate. J Geophys Res 102:3761–3778

Chylek P, Coakley JA (1974) Aerosols and climate. Science 183:75–77

Chylek P, Wong J (1995) Effect of absorbing aerosols on global radiation budget. Geophys Res Lett 22:929–931

Cooke WF, Wilson JJN (1996) A global black carbon aerosol model. J Geophys Res 101:19 395–19 410

d'Almedia GA, Koepke P, Shettle EP (1991) Atmospheric aerosols: global climatology and radiation characteristics. A Deepak Publishing, Hampton, VA, USA

Fenn RW, Clough SA, Gallery WO, Good RE, Kneizys FX, Mill JD, Rothman LS, Shettle EP, Volz FE (1985) Optical and infrared properties of the atmosphere. In: Jursa AS (ed) Handbook of geophysics and the space environment. Air Force Geophysics Laboratory

Grant KE Grossman AS (1998) Description of a solar radiative transfer model for use in LLNL climate and atmospheric chemistry studies. Lawrence Livermore National Laboratory Report UCRL-ID-129949

Grant KE, Grossman AS, Chuang CC, Penner JE (1996) Sensitivity of aerosol radiative forcing calculations to spectral resolution. Proc 1996 Int Radiation Symp, 19–24 August, 1996, Fairbanks, AK, pp 275–278

Gray HA, Cass GR, Huntzicker JJ, Heyerdahl EK, Rau JA (1984) Elemental and orgnaic carbon particle concentrations: a long-term perspective. Sci Total Environ 36:17–25

Groblicki PJ, Wolff GT, Countess RJ (1981) Visibility-reducing species in the Denver "brown cloud" - I. Relationships between extinction and chemical composition. Atmos Environ 15:2473–2484

Haywood JM, Shine KP (1995) The effect of anthropogenic sulfate and soot aerosol on the clear sky planetary radiation budget. Geophys Res Lett 22 : 603–606

Haywood JM, Ramaswamy V, Donner LJ (1997) A limited-area-model case study of the effects of sub-grid scale variations in relative humidity and cloud upon the direct radiative forcing of sulfate aerosol. Geophys Res Lett 24 : 143–146

Haywood JM, Ramaswamy V (1998) Global sensitivity studies of the direct radiative forcing due to anthropogenic sulfate and black carbon aerosols. J Geophys Res 103 : 6043–6058

Hegg DA, Livingtson J, Hobbs PV, Novakov T, Russell P (1997) Chemical apportionment of aerosol column optical depth off the mid-Atlantic coast of the United States. J Geophys Res (in press)

Hobbs PV, Reid JS, Kotchenruther RA, Ferek RJ, Weiss R (1997) Direct radiative forcing by smoke from biomass burning. Science 275 : 1777–1778

Horvath H (1993) Atmospheric light absorption – a review. Atmos Environ 27 : 293–318

IPCC (1996) Climate change 1995: the science of climate change. In: Houghton JT, Meira Filho LG, Callander BA, Harris N, Kattenberg A, and Maskell K (eds) Cambridge University Press, Cambridge, UK

Japar SM, Brachaczek WW, Gorse RA Jr, Norbeck JM, Pierson WR (1986) The contribution of elemental carbon to the optical properties of rural atmospheric aerosols. Atmos Environ 20 : 1281–1289

Kiehl JT, Briegleb BP (1993) The relative role of sulfate aerosols and greenhouse gases in climate forcing. Science 260 : 311–314

Kiehl JT, Rodhe H (1995) Modeling geographical and seasonal forcing due to aerosols. In: Charlson RJ, Heintzenberg J (eds) Aerosol forcing of climate. John Wiley and Sons, Chichester, pp 281–296

Mitchell JFB, Johns TC, Gregory JM, Tett SFB (1995) Climate response to increasing levels of greenhouse gases and sulphate aerosols. Nature 376 : 501–504

Liou K-N (1980) An introduction to atmospheric radiation. Academic Press, Orlando, Florida, 392 pp

Liousse C, Penner JE, Chuang CC, Walton JJ, Eddleman H, Cachier H (1996) A three-dimensional model study of carbonaceous aerosols. J Geophys Res 101 : 19 411–19 432

Lohmann U, Feichter J (1997) Impact of sulfate aerosols on albedo and lifetime of clouds: a sensitivity study with the ECHAM4 GCM. J Geophys Res 102 : 13 685–13 700

Nemesure S, Wagener R, Schwartz SE (1995) Direct shortwave forcing of climate by anthropogenic sulfate aerosol: sensitivity to particle size, composition, and relative humidity. J Geophys Res 100 : 26 105–26 116

Novakov T, Corringa CE (1996) Influence of sample composition on aerosol organic and black carbon determinations. In: Levine J (ed) Biomass burning and global change vol 1. MIT Press, Cambridge, MA, pp 531–539

Penner JE, Dickinson R, O'Neill C (1992) Effects of aerosol from biomass burning on the global radiation budget. Science 256 : 1432–1434

Penner JE, Eddleman H, Novakov T (1993) Towards the development of a global inventory of black carbon emissions. Atmos Environ 27A : 1277–1295

Penner JE, Atherton CA, Graedel TE (1994) Global emissions and models of photochemically active compounds. In: Prinn R (ed) Global atmospheric-biospheric chemistry. Plenum Publishing, NY, pp 223–248

Penner JE (1995) Carbonaceous aerosols influencing atmospheric radiation: black and organic carbon. In: Charlson RJ, Heintzenberg J (eds) Aerosol forcing of climate. John Wiley and Sons, Chichester pp 91–108

Penner JE, Chuang CC, Liousse C (1996) The contribution of carbonaceous aerosols to climate change. In: Kulmala M, Wagner PE (eds) Nucleation and atmospheric aerosols 1996. Elsevier Science, pp 759–769

Penner JE, Wigley TML, Jaumann P, Santer BD, Taylor KE (1997a) Anthropogenic aerosols and climate change: a method for calibrating forcing. In: Howe W, Henderson-Sellers A (eds) Assessing climate change: results from the model evaluation consortium for climate assessment. Gordon and Breach Science Publishers, Sydney, Australia, pp 91–111

Penner JE, Pan W, Jacobson MZ (1997b) Climate forcing by anthropogenic aerosols: Nonlinear impacts from nitrate and ammonium, 1997 AGU Spring Meeting Abstr. p S64

Pereira EB, Setzer AW, Gerab F, Artaxo PE, Pereira MC, Monroe G (1996) Airborne measurements of aerosols from burning biomass in Brazial related to the TRACE A experiment. J Geophys Res 101 : 23 983–23 992

Pilinis C, Pandis SN, Seinfeld JH (1995) Sensivity of direct climate forcing by atmospheric aerosols to aerosol size and composition. J Geophys Res 100 : 18 739–18 754

Pruppachter HR Klett JD (1978) Microphysics of clouds and precipitation. D Reidel, Dordrecht Boston London, 714 pp

Radke LF, Hegg DA, Lyons JH, Brock CA, Hobbs PV, Weiss R, Rasmussen R (1988) Airborne measurements on smokes from biomass burning. In: Hobbs PV, McCormick MP (eds) Aerosols and climate. A Deepak Publishing, Hampton, VA pp 411–422

Roeckner E, Siebert T, Feichter J (1996) Climatic response to anthropogenic sulfate forcing simulated with a general circulation model. In: Charlson RJ, Heintzenberg J (eds) Aerosol forcing of climate. John Wiley and Sons, Chichester pp 349–362

Rogge WF, Hildemann LM, Mazurek MA, Cass GR (1993) Sources of fine organic aerosol. 4. Particulate abrasion products from leaf surfaces of urban plants. Environ Sci Technol 27 : 2700–2711

Schult I, Feichter J, Cooke WF (1997) Effect of black carbon and sulfate aerosols on the global radiation budget. J Geophys Res 203 : 30,107–30,117

Sloane CS, Richards LW (1991) Size-segregated fine particle measurements by chemical species and their impact on visibility impairment in Denver. Atmos Environ 25A : 1013–1024

Stocks B (1991) The extent and impact of forest fires in northern circumpolar countries (1991) In: Levine J (ed) Global biomass burning. MIT Press, Cambridge, MA pp 197–202, 1991

Taylor KE, Ghan SJ (1992) An analysis of cloud liquid water feedback and global climate sensitivity in a general circulation model. J Clim 5 : 907–919

Taylor KE, Penner JE (1994) Response of the climate system to atmospheric aerosols and greenhouse gases. Nature 369 : 734–737

Toon OB, Pollack JB, Khare BN (1976) The optical constants of several atmospheric aerosol species: ammonium sulfate, aluminum oxide, and sodium chloride. J Geophys Res 81 : 5733–5748

Vose MM, Swank WT, Geron CD, Major AE (1996) Emissions from forest burning in the Southeastern United States: application of a model determining spatial and temporal fire variation. In: Levine J (ed) Biomass burning and global change, vol 2. MIT Press, Cambridge, MA pp 733–749

Wang X, Feng Z, Zhuang Y (1996) Forest fires in China: carbon dioxide emissions to the atmosphere. In: Levine J (ed) Biomass burning and global change vol 2. MIT Press, Cambridge, MA pp 771–779

Williamson DL, Kiehl JT, Ramanathon V, Dickinson RE, Hack JJ (1987) Description of NCAR community climate model (CCM1). NCAR Tech Note NCAR/TN-285 + STR, Natl Cent for Atmos Res, Boulder, CO 112pp

Zhang X, Turpin BJ, McMurry PH, Hering SV, Stolzenburn MR (1994) Mie theory evaluation of species contributions to 1990 wintertime visibility reduction in the Grand Canyon. J Air Waste Manage Assoc 44 : 153–162